View metadata, citation and similar papers at core.ac.uk
brought to you by CORE
provided by Repository@Nottingham

Journal of Applied Physics
ACCEPTED MANUSCRIPT
AIP Publishing
This is the author's peer reviewed, accepted manuscript. However, the online version of record will be different from this version once it has been copyedited and typeset.
PLEASE CITE THIS ARTICLE AS DOI: 10.1063/1.5140447

# Effect of thermal annealing on the optical and structural properties of (311)B and (001) GaAsBi/GaAs single quantum wells grown by MBE

**Haifa Alghamdi[1,2*], Vanessa Orsi Gordo[3], M. Schmidbauer[4], Jorlandio F. Felix[5], Sultan Alhassan[1], Amra Alhassni[1], Gabriela Augusta Prando[3], Horácio Coelho-Júnior[6], M. Gunes[7], Helder Vinicius Avanço Galeti[8], Yara Galvão Gobato[3], Mohamed Henini[1]**

[1*]School of Physics and Astronomy, University of Nottingham, Nottingham NG7 2RD, UK
[2]Physics Department, Faculty of Sciences - AL Faisaliah, University of Jeddah, Ministry of Education Kingdom of Saudi Arabia, Jeddah, 21959, Saudi Arabia
[3]Departamento de Física, Universidade Federal de São Carlos (UFSCar) 13565-905, São Carlos, SP, Brazil
[4]Leibniz-Institut für Kristallzüchtung, Max-Born-Straße 2, 12489 Berlin, Germany
[5]Universidade de Brasília, Instituto de Física, Núcleo de Física Aplicada, Brasília DF 70910-900, Brazil
[6]Centro Brasileiro de Pesquisas Físicas, Rua Dr. Xavier Sigaud 150, Urca, 22290-180 Rio de Janeiro, RJ, Brazil
[7]Department of Materials Engineering, Engineering Faculty, Adana Alparslan Turkes Science and Technology University, 01250 Adana, Turkey
[8]Departamento de Engenharia Elétrica, Universidade Federal de São Carlos (UFSCar) 13565-905, São Carlos, SP, Brazil

Contact author: *Haifa.Alghamdi@nottingham.ac.uk

## Abstract

The effect of Furnace Annealing (FA) and Rapid Thermal annealing (RTA) on the structural and optical properties of $GaAs_{1-x}Bi_x$/GaAs single quantum wells (SQW) grown on (001) and (311)B substrates by molecular beam epitaxy (MBE) was investigated. The structural properties were investigated by high-resolution X-ray diffraction (HR-XRD) and Transmission Electron Microscopy (TEM). The Bi concentration profiles were determined by simulating the HR-XRD 2θ-ω scans using dynamical scattering theory to estimate the Bi content, lattice coherence and quality of the interfaces. The Bi composition was found to be similar for both samples grown on (001) and (311)B GaAs substrates. However, the simulations indicate that the Bi composition is not only limited in the GaAsBi QW layer but extends out of the GaAsBi QW towards the GaAs barrier. Photoluminescence (PL) measurements were performed as a function of temperature and laser power for samples with a nominal Bi composition of 3%. PL spectra showed that (001) and (311)B samples have different peak energies at 1.23 eV and 1.26 eV, respectively, at 10 K. After RTA at 300 °C for 2 mins, the PL intensity of (311)B and (001) samples was enhanced by a factor of ~2.5 and 1.75, respectively. However, for the (001) and (311)B FA samples an enhancement of the PL intensity by a factor of only 1.5 times could be

ACCEPTED MANUSCRIPT
Journal of Applied Physics
AIP Publishing
This is the author's peer reviewed, accepted manuscript. However, the online version of record will be different from this version once it has been copyedited and typeset.
PLEASE CITE THIS ARTICLE AS DOI: 10.1063/1.5140447

achieved. The enhancement of PL intensity in annealed samples was interpreted in terms of PL activation energies, with a reduction of the alloy disorder and an increase of the Bi cluster.

**Keywords:** GaAsBi; Single quantum wells; Molecular beam epitaxy; Photoluminescence; X-ray diffraction; Transmission Electron Microscopy.

## 1. Introduction

Recently, dilute bismide alloys grown on GaAs have attracted much attention due to their physical properties and potential applications in photonic devices and long–wavelength optoelectronics [1,2]. The incorporation of a few atomic percent of Bi into GaAs (substitution of As atoms with Bi atoms) strongly affects the properties of GaAs. For example, a giant band gap bowing effect was observed leading to a strong reduction of the band gap energy by 88meV per % Bi [1]. In addition, the increase of the spin-orbit (SO) splitting energy with Bi concentration [3, 4] makes GaAsBi-based structures suitable for spintronic applications [3, 51]. Furthermore, due to the relatively large size of bismuth atoms, a strong deformation of the GaAs lattice occurs producing an increase of the carrier-phonon coupling [5]. However, incorporation of Bi into GaAs causes a strong effect on the carrier recombination processes due to an increase of the density of the localized states [6-8]. As a result of this effect, an extension of the band-edge toward lower energies, the so-called band-tail states is created [9]. The localized states in GaAsBi are attributed to the variations of the alloy composition together with clustering of Bi [10]. Mostly, the effects of localization on the system lead to considerable changes in carrier dynamics, therefore affecting the performance of optoelectronic devices.

Most of the research on GaAsBi has mainly been devoted to films which have been grown on conventional GaAs (001) substrate [11-14], however, there are very few reports on GaAsBi structures grown on high-index surfaces [15, 16]. Bi concentrations as high as 22% have been achieved in GaAs [13]. Besides, the optical and structural properties of (001) GaAsBi/GaAs single [17- 19] and multi-quantum wells (QWs) [20, 21], and (411) [22] and (311)B GaAs substrates [23-24] have been reported.

In order to substitute As atoms with Bi atoms in GaAs, GaAsBi alloys are grown at low temperatures ($T_G$ = 200 °C - 400 °C) because Bi atoms are much bigger than As atoms. However, adopting this unconventional growth regime to incorporate Bi into the host GaAs lattice creates structural defects which behave as nonradiative centers such as native point defects and clusters [25] affecting their optical efficiency. It is well-known that post-growth

ACCEPTED MANUSCRIPT
Journal of Applied Physics
AIP Publishing
This is the author's peer reviewed, accepted manuscript. However, the online version of record will be different from this version once it has been copyedited and typeset.
PLEASE CITE THIS ARTICLE AS DOI: 10.1063/1.5140447

thermal treatment improves the optical properties of semiconductor structures by dissociating complex defects and annihilating some other non-radiative recombination centers in order to reduce their concentrations. At the same time, the incorporated Bi atoms often segregate and form Bi-rich clusters with various structures sizes in the range of 5–20 nm during thermal annealing process, depending on the Bi content and on the annealing conditions [50].

The aim of this work is to investigate the effect of two thermal annealing processes on the optical and structural properties of GaAsBi/GaAs QWs. Previous studies have shown an improvement of the PL peak intensity in lattice mismatched dilute nitride GaAsN/GaAs materials by using RTA [26, 27]. The influence of thermal annealing was also investigated in dilute bismide III-V materials both in bulk and QW structures grown by MBE on (001) GaAs substrates [18, 28- 30, 52] using RTA. Most of the reported work on annealing was carried out at very high temperatures above the growth temperature of the samples. However, J.F. Rodrigo et al [16] reported that (311)B GaAsBi layers grown at 350 ºC and annealed at 200 ºC for 3 hours resulted in a decrease of the structural defects in the epilayer with a huge increase of the photoluminescence signal. It is worth pointing out that the influence of annealing procedures on the optical and structural properties of MBE grown GaAsBi QWs have not been reported as a function of substrate orientation.

In this paper, we study the effect of thermal annealing temperatures, annealing times and thermal annealing techniques on the optical and the structural properties of a $GaAs_{(1-x)}Bi_x$/GaAs single QW grown at 320 °C by MBE on semi-insulating (001) and (311)B GaAs substrates with a nominal Bi content x = 3%. The approach adopted for the annealing process was the use of low and high temperatures for long and short annealing times, respectively. The best material quality was obtained by annealing at 300 °C and 2 minutes using RTA. The electronic band-profiles are calculated using the vertical Bi profile which were determined by simulating the high-resolution X-ray diffraction (HR-XRD) data using dynamical scattering theory. Correlations between HR-XRD and TEM results will be discussed.

## 2. Method and Experimental details

In order to substitute As atoms with Bi atoms in GaAs, GaAsBi alloys are usually grown at low temperatures between 200 °C - 400 °C because Bi atoms are much bigger than As atoms. This means that the incorporation of Bi into the GaAs lattice is enhanced at growth temperatures lower than 400 °C. In this work the growth of GaAsBi single quantum well (SQW) samples started with the deposition of a 370 nm GaAs buffer layer. The first 300 nm

ACCEPTED MANUSCRIPT
Journal of Applied Physics
AIP Publishing
This is the author's peer reviewed, accepted manuscript. However, the online version of record will be different from this version once it has been copyedited and typeset.
PLEASE CITE THIS ARTICLE AS DOI: 10.1063/1.5140447

was grown at high As overpressure and at a temperature of 580 °C which the optimum growth temperature of GaAs. The growth temperature of GaAs was then lowered from 580 °C to 320 °C for the last 70 nm before the growth of GaAsBi QW in order to reach the growth temperature for optimum incorporation of Bi into GaAs. This was followed by a 10 nm thick GaAsBi SQW layer and a 50 nm GaAs cap grown at the same temperature (see Figure 1). The growth rate was ~ 0.4µm/h for all layers. For efficient Bi incorporation, the atomic Ga/As flux ratio was adjusted close to the stoichiometric value before the growth of the QW. All our samples were grown using $As_4$ species.

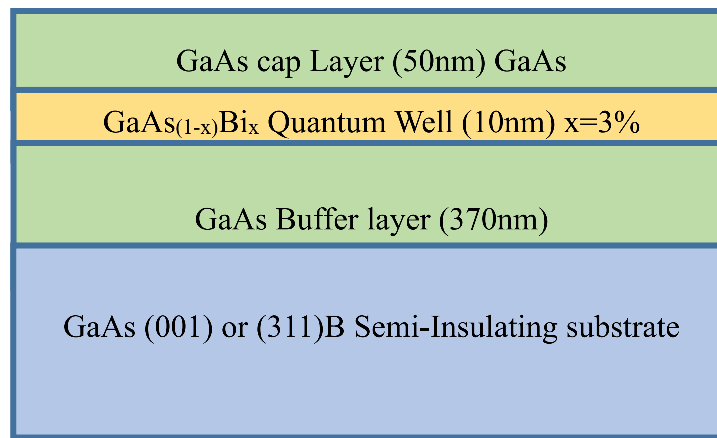


Figure 1: Schematic diagram of GaAsBi/GaAs SQW sample grown on (001) and (311)B GaAs substrates.

The effect of Bi localization due to alloy fluctuations and clustering on the optical properties is investigated for dilute bismuth GaAsBi QWs using PL measurements as a function of temperature and excitation power. A 532 nm green laser is used as an excitation power ($P_{EXC}$) source ranging from 0.5 mW to 33 mW. All samples were checked for uniformity before annealing them using PL measurements. The PL energy and PL intensity were similar at different positions in the sample. The size of the original samples were 8×8 $mm^2$ squares. These were cleaved into four pieces for different annealing treatments.

For this purpose, we have applied RTA at different temperatures and durations (500 °C for 1min, 300 °C for 2mins and 700 ºC for 30 sec) and FA in a tubular furnace at 200 °C for 3h. All heat treatments were carried out under $N_2$ gas conditions. It is worth pointing out that the samples were placed between two protective GaAs substrates in order to avoid As evaporation from the top GaAs cap layer and formation of Ga droplets.

ACCEPTED MANUSCRIPT
Journal of Applied Physics
AIP Publishing
This is the author's peer reviewed, accepted manuscript. However, the online version of record will be different from this version once it has been copyedited and typeset.
PLEASE CITE THIS ARTICLE AS DOI: 10.1063/1.5140447

The PL measurements were performed at temperatures between 10 and 300 K using a high-resolution optical spectrometer, an InGaAs dual detector, and a computer-controlled lock-in amplifier.

To gain an insight into the evolution of the structural properties of the samples upon annealing, a Bruker D8 Discover HR-XRD diffractometer system was used. An asymmetric 2-bounce Ge 220 channel-cut monochromator was used to select the Cu Kα1 line at λ= 1.540 56 Å and to collimate the incident X-ray beam. Symmetrical 2θ-ω scans were performed from which the layer thicknesses, vertical strains and vertical Bi concentration profiles were determined.

Cross-sectional TEM specimens were prepared using a Focused Ion Beam (FIB), model Quanta FEG 3D FEI. Before FIB sample preparation, the surface of the sample was coated with a platinum film to prevent the surface from bombardment by the ion beam. The samples were investigated with a FEI Tecnai G2-20 Super-Twin transmission electron microscope operated at 200 kV of acceleration voltage.

## 3. Results and Discussion

### 3.1. Structural Properties

HR-XRD diffraction curves (2θ-ω scans) are shown in Figure 2. The sharp peaks at about 2θ = 66.05° and 53.73° are the GaAs (004) and (311) substrate Bragg reflections, respectively. In both cases, we observe a weak shoulder at low angle side of the strong substrate Bragg reflections which can be attributed to the compressively strained GaAsBi QWs. However, the well-defined intensity fringes around the sharp substrate Bragg peaks clearly prove a smooth interface between the epitaxial layer and the substrate.

In order to evaluate the vertical Bi concentration profiles, the experimental diffraction curves were simulated using dynamical scattering theory. In these simulations we have determined the Bi concentration through a linear interpolation between the lattice parameters of GaAs (a = 5.653 Å) and of a hypothetical zincblende GaBi (a = 6.33 Å) [53]. Linear elasticity theory has been applied. Owing to the low Bi content we have used, as a good approximation, throughout the elastic coefficients of GaAs [54].

The best fits, which are in excellent agreement with the experimental data, are shown as solid lines in Figure 2. It is worth noting that the obtained Bi concentration profiles shown in Figure 2 contain a number of fitting parameters making the fitting routine presumably not reliable. For that reason we have performed many extended simulations in which we tried to further refine the simulations. In all of these simulations we obtained very similar Bi concentration profiles. The simulations show that the maximum Bi concentrations in the QWs are 2.15% and

ACCEPTED MANUSCRIPT
Journal of Applied Physics
AIP Publishing
This is the author's peer reviewed, accepted manuscript. However, the online version of record will be different from this version once it has been copyedited and typeset.
PLEASE CITE THIS ARTICLE AS DOI: 10.1063/1.5140447

2.10% for the samples grown on (001) and (311)B substrates, respectively. However, as seen in the inset of Figure 2, the Bi content spreads out from the GaAsBi QW to the GaAs cap. Therefore, for both samples, the total thickness of the Bi-containing layer is much larger than the nominal GaAsBi QW thickness. Since the GaAs cap was grown at the same temperature as the GaAsBi QW, it can be assumed that the Bi atoms on the surface continue to incorporate after the nominal QW growth. The thickness of the Bi containing layers is almost the same for both samples; however, the amount of Bi in the extended/top layer region in the sample grown on (311)B GaAs is higher than that in the sample grown on (001) GaAs.

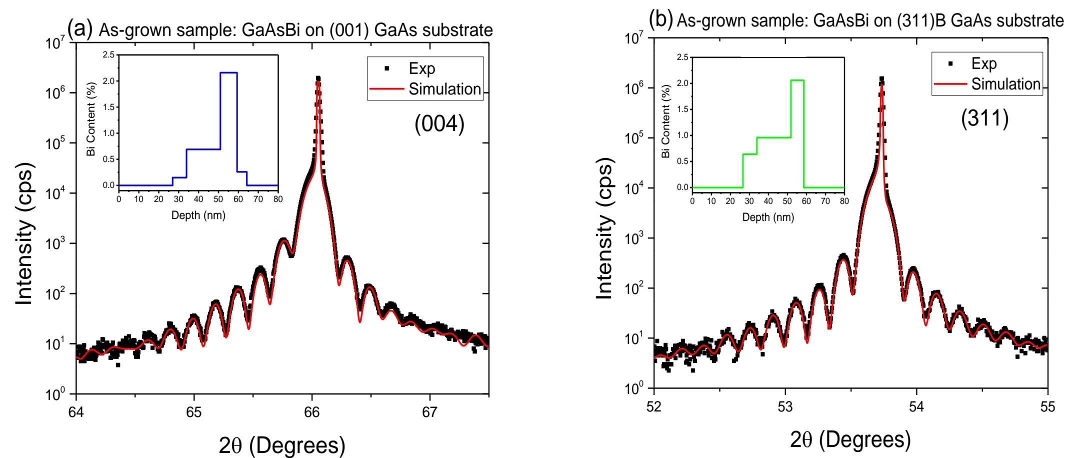


Figure 2. Experimental (black dots) and simulated (solid lines) 2θ-ω scans of samples grown on (a) (001) GaAs and (b) (311)B GaAs substrates. The insets show the vertical Bi concentration profile which was used in the simulations. Reproduced with permission from Semiconductor Science and Technology 33, 124015 (2018). ©IOP Publishing. Reproduced with permission. All rights reserved

Figure 3 shows HR-XRD 2θ-ω scans obtained for samples grown on (001) and (311)B GaAs substrates which were RTA annealed at 300 ºC for 2 mins. As can be seen for both growth on (001) and (311)B GaAs, the as-grown and annealed samples show only very small differences. The corresponding X-ray simulations (not shown here) support this statement: The vertical Bi-concentration profiles displayed in the inset of Figure 3 are essentially identical.

ACCEPTED MANUSCRIPT
Journal of Applied Physics
AIP Publishing
This is the author's peer reviewed, accepted manuscript. However, the online version of record will be different from this version once it has been copyedited and typeset.
PLEASE CITE THIS ARTICLE AS DOI: 10.1063/1.5140447

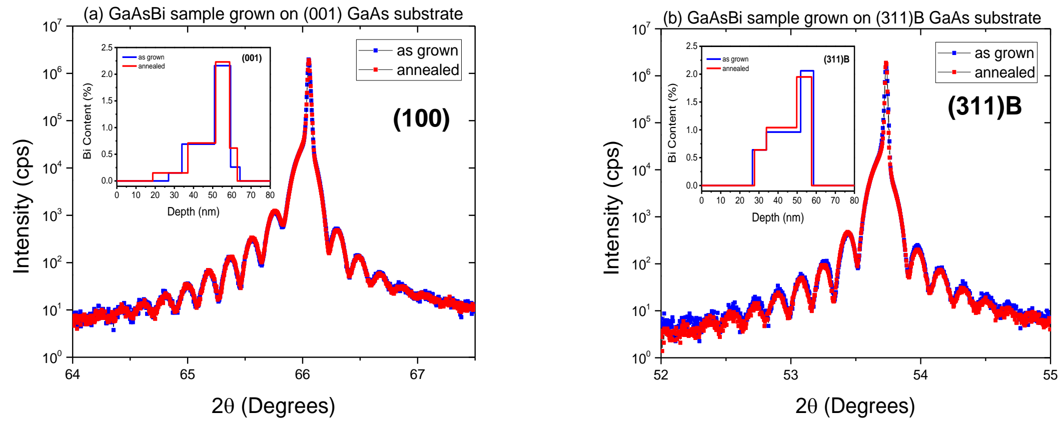


Figure 3. 2θ-ω scans of as-grown and RTA annealed samples around the symmetrical (a) (004) and (b) (311)B Bragg reflections of the GaAs substrate. The corresponding insets show the Bi concentration profiles used in the best data fits for all four samples.

The HR-XRD studies described above show no measurable impact of annealing on the vertical Bi-concentration profile. In the X-ray measurements, however, a lateral averaging over large sample areas of typically a few $mm^2$ is carried out. Therefore, possible Bi clustering may not be directly visible in the X-ray data. In order to obtain local information on atomic scale high-resolution. For that reason high-resolution TEM measurements were performed in order to obtain local structural information on the atomic scale.

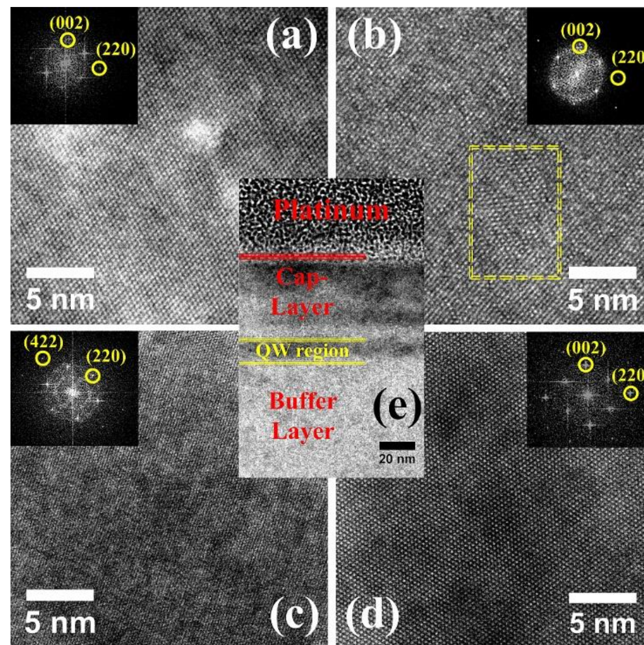


Figure 4. High-Resolution TEM micrographs obtained from the GaAsBi/GaAs interface region: (a) as-grown (001) sample, (b) annealed (001) sample, (c) as-grown (311)B sample and

ACCEPTED MANUSCRIPT
Journal of Applied Physics
AIP Publishing
This is the author's peer reviewed, accepted manuscript. However, the online version of record will be different from this version once it has been copyedited and typeset.
PLEASE CITE THIS ARTICLE AS DOI: 10.1063/1.5140447

(d) annealed (311)B sample. In (a), (b) and (d), the insets show the results of the fast Fourier transform (FFT) image reconstructions along the [110] zone axis, respectively, while in (c) the FFT image is along the [$\bar{1}$11] zone axis. The dashed line in (b) indicates a region of structural relaxation after annealing. (e) annealed (311)B sample at lower magnification; the sample surface is between platinum and cap-layer. The substrates are located on the bottom of image (a) an (b) and left side of image (c) and (d).

Figures 4 (a)-(d) display HRTEM micrographs of the GaAs/GaAsBi interface of the as-grown and annealed (300 ºC for 2 mins) samples. We performed a calibration procedure independently for the (220) planes of the GaAs substrates, and they all agree very well, showing only a very small deviation less than 0.3% between theoretical and measured value. It is important to notice that all micrographs have the same magnification. As can be seen from the figures, dark regions between bright regions in all images are observed, which could be interpreted as clusters based on Bi atoms. Additionally, the main difference between the micrographs is the contrast of dark regions. This characteristic is an indication of different distributions of Bi atoms in the materials structure. Figure 4(e) shows the cross-sectional TEM micrograph of the annealed (311)B sample. We can clearly observe the formation of a layered structure as schematically sketched in Figure 1 (capping layer/QW/Buffer layer). The thickness of the GaAs capping layer is ~50 nm, while the QW region is ~ 10 nm thick.

Figures 4(a) and 4(b) are HRTEM images from as-grown and annealed samples grown on (001) GaAs substrates, respectively. The area represented by the dashed rectangular shown in Figure 4(b) provides a strong indication of Bi clustering of about 10 nm in size, probably due to the Bi-segregation during annealing. This characteristic has been observed also in the work of Baladés et al [31]. In this paper, the authors reported the Bi distribution in epitaxial GaAsBi-on-GaAs by using High Angle Annular Dark-Field Scanning Transmission Electron Microscopy (HAADF-STEM) technique. They reported a non-homogeneous Bi distribution at the interfaces as well as within the GaAsBi layer. In that case the clusters may lead to a partially relaxed GaAsBi/GaAs system around them. However, in our samples we identify in Figure 4 (b) a structural disorder due to annealing that can be attributed to the Bi-segregation followed by a structural relaxation in the QW region. This evidence is compelling if we compare Figures4 (c) with 4 (d): the distributions of dark regions are more disperse in (c), but after annealing a major separation of these dark regions is observed that correspond to Bi-segregation. As can be seen from these HRTEM images, it is not possible to identify structural defects such as extended defects. Finally, the results indicated that the Bi clusters segregation

ACCEPTED MANUSCRIPT
Journal of Applied Physics
AIP Publishing
This is the author's peer reviewed, accepted manuscript. However, the online version of record will be different from this version once it has been copyedited and typeset.
PLEASE CITE THIS ARTICLE AS DOI: 10.1063/1.5140447

is more pronounced in (001) samples after annealing [Figure 4(b)]. This event can be associated with Bi clusters reported by Beladés et al [31]. Nevertheless, corroborating with HR-XRD, the GaAs buffer layer is not visible in the TEM images indicating, therefore, the existence of the same vertical lattice parameter than that from GaAs substrate.

#### 3.2.3.2 Optical Properties

Figure 5 shows normalized PL spectra conducted at 10K for the as-grown samples grown on both the (001) and (311)B GaAs surface orientations. The PL spectra show a similar asymmetric shape for both samples, while the energy peak of the high index (311)B plane sample is less shifted than (001) oriented sample by 32 meV. Although the sample grown on (001) plane has a slightly higher content of Bi (0.05%) in the QW layer, as compared to (311)B sample and confirmed by HR-XRD results, this feature does not explain the energy difference observed in the PL peak. However, it is difficult to compare straight the PL of (001) sample with (311)B because the latter has more spatial variations in Bi incorporation. This may be due to more clustering of Bi and carrier localization at Bi pairs and clusters [32, 33]. This feature seems to affect the PL peak intensity which is 9 times higher in (001) sample than in (311)B sample, probably due to a smaller amount of non-radiative defects *in (001) sample [11].* It is important to point out that the quantum confinement could affect the PL peak position but less than Bi content, since the nominal QW width is around 10 nm. Furthermore, the Bi segregation from the GaAsBi QW to the GaAs cap could lead to a larger QW width and therefore there is a reduction of quantum confinement. In addition, the reduction of the band gap energy seems be higher in (001) than in (311)B sample, resulting in a less energetic PL peak. Therefore, it is very difficult to separate all effects that contribute to the observed difference in the PL peak in this case.

ACCEPTED MANUSCRIPT
Journal of Applied Physics
AIP Publishing
This is the author's peer reviewed, accepted manuscript. However, the online version of record will be different from this version once it has been copyedited and typeset.
PLEASE CITE THIS ARTICLE AS DOI: 10.1063/1.5140447

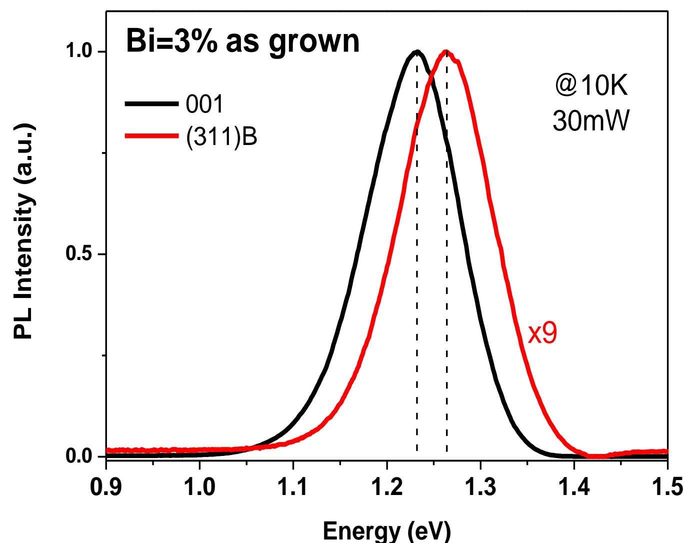


Figure 5. Normalised PL spectra for as-grown samples on (001) and (311)B GaAs substrate.

The excitation power dependence of the PL spectra has been investigated in detail. Figure 6 shows the normalized PL spectra for the QW samples at 10K as a function of the excitation laser power ($P_{EXC}$) from 0.5mW to 33mW for (a) (001) and (b) (311)B samples. As can be seen from Figure 6(c), the PL peak exhibits a blue shift with increasing $P_{EXC}$ indicating the appearance of carrier localization. However, for $GaAs_{(1-x)}Bi_x$ it is well-known that this effect is due to the occurrence of localized states near the top of the valence band. As explained previously, such localized states are expected to form in the regions with higher local Bi concentrations, which can be due to Bi clusters and Bi-related defects.

ACCEPTED MANUSCRIPT
Journal of Applied Physics
AIP Publishing
This is the author's peer reviewed, accepted manuscript. However, the online version of record will be different from this version once it has been copyedited and typeset.
PLEASE CITE THIS ARTICLE AS DOI: 10.1063/1.5140447

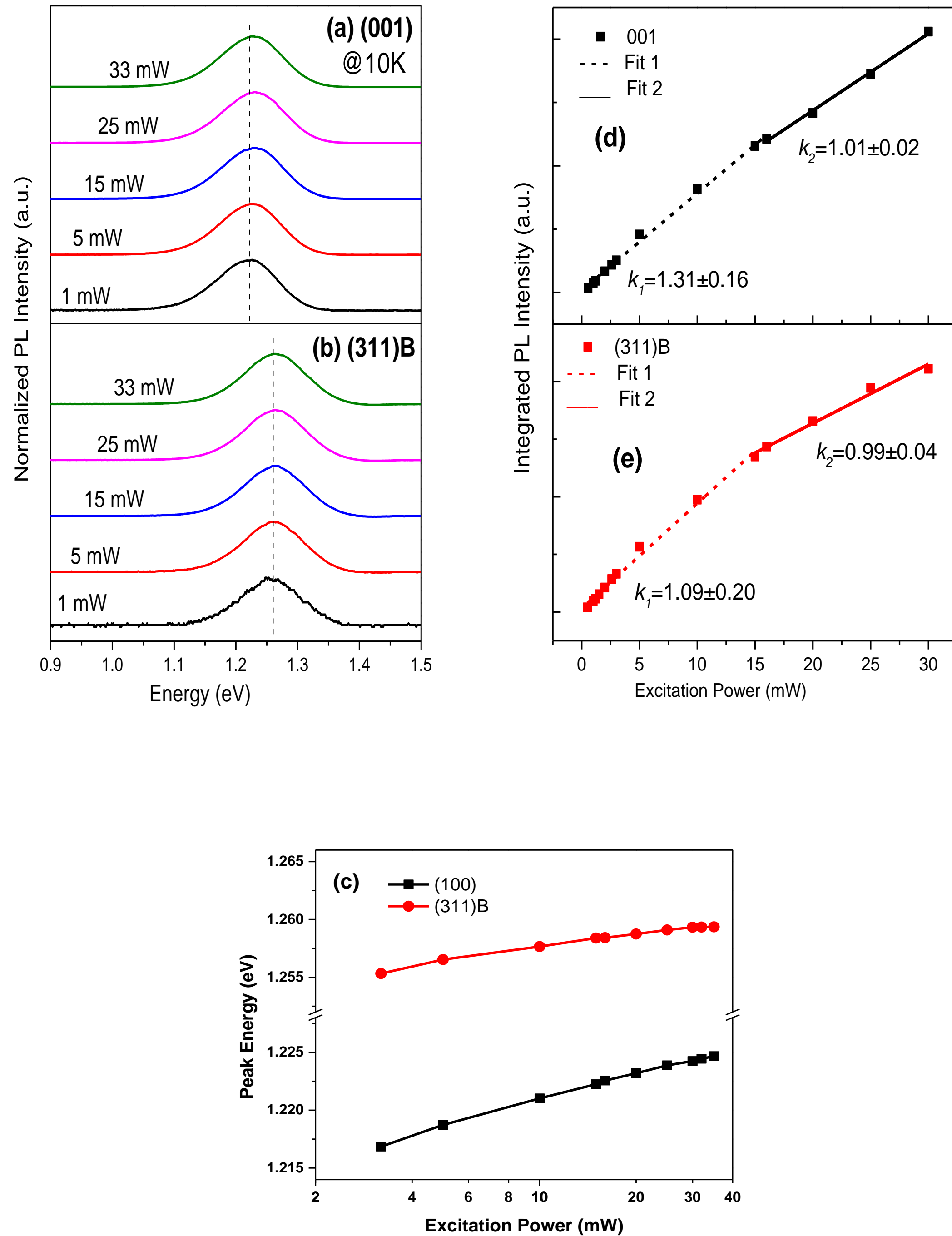


Figure 6. Normalized PL spectra at 10 K for different $P_{EXC}$ for (a) (001) and (b) (311)B as-grown samples. (c) PL peak energy as a function of $P_{EXC}$ for (001) and (311)B samples. Integrated PL intensity (IPL) as a function of $P_{EXC}$ for (d) (001) and (e) (311)B samples at 10K. The solid and dashed lines represent the fitting using equation: $I_{PL} = \beta P_{EXC}^{k}$

As illustrated in Figure 6 (c), by increasing $P_{EXC}$ from 3.2 mW to 35mW, the maxima of the QW PL spectra, $E_{max}$, of (001) and (311)B samples undergoes a small blue-shift from 1.217 to

ACCEPTED MANUSCRIPT
Journal of Applied Physics
AIP Publishing
This is the author's peer reviewed, accepted manuscript. However, the online version of record will be different from this version once it has been copyedited and typeset.
PLEASE CITE THIS ARTICLE AS DOI: 10.1063/1.5140447

1.225 eV and from 1.255 to 1.259eV, respectively. These peaks correspond to excitation ground-state recombination in the QW.

To analyse the emission from the (001) and (311)B samples, the integrated PL intensity was plotted as a function of excitation power as shown in Figure 6 for (d) (001) and (e) (311)B samples. The solid and dashed lines represent the fitting curves using the power law $I_{PL} = \beta P_{EXC}^{k}$ [34]. $I_{PL}$ is the integrated PL intensity and β and k are fitting parameters. Two k values ($k_1$ and $k_2$) for each sample were obtained, indicating two different processes for carrier radiative recombination as a function of $P_{EXC}$.

As shown in Figure 6 (c), the PL peak has the lowest energy at low $P_{EXC}$. Under this low power excitation, the PL emission is controlled by radiative recombination of carriers that occupy localized states close to the valence band maximum. For both samples, the value of $k_1$ is > 1 indicating that both free excitons and free carriers contribute the recombination process. However, as $P_{EXC}$ increases to a high-power regime, the obtained value of $k_2$ is ~1, lower than $k_1$. This means that as the $P_{EXC}$ is increased, the recombination process, which is limited by nonradiative recombination centres, is dominated by free excitons. This effect could be due to the fact that the localized states are being fully occupied by carriers and a strong evidence of this effect is demonstrated by a blueshift of the PL peak as $P_{EXC}$ is increased as shown in figure 6 (c) [17, 35, 36].

The temperature dependence of PL spectra of (001) and (311)B samples are shown in Figure 7. Both samples exhibit a redshift of the PL peak as the temperature is increased. This well-known effect is due to the dependence of the bandgap energy with temperature. However, alloy disorder and potential fluctuations are the main cause of exciton localization. In this case, the temperature dependence of the PL peak position cannot be accounted for by using the standard Varshni's model [37]. The well-known 'S-shaped' behaviour observed in disordered semiconductors such as GaAsN and GaAsBi could possibly explain this effect [36, 38, - 40]. It has been reported that the PL spectra are dominated by free excitons at high $P_{EXC}$ and temperature conditions [17, 35, 36]. As shown in Figure 7 (c-d), the PL peak red-shits and the PL FWHM gets larger as the temperature is increased. There is no clear evidence of S-shape behaviour in these samples. This could be due to the use of high $P_{EXC}$ that could make this effect less evident since the localized states are completely filled in this condition. Mazur et al also have shown that by increasing excitation intensities the S-shape becomes less noticeable, and for high power the S-shape vanishes completely [41]. Similar reported results on PL of GaAsBi QWs grown on (001) GaAs substrates [38, 42] are in good agreement with ours.

ACCEPTED MANUSCRIPT
Journal of Applied Physics
AIP Publishing
This is the author's peer reviewed, accepted manuscript. However, the online version of record will be different from this version once it has been copyedited and typeset.
PLEASE CITE THIS ARTICLE AS DOI: 10.1063/1.5140447

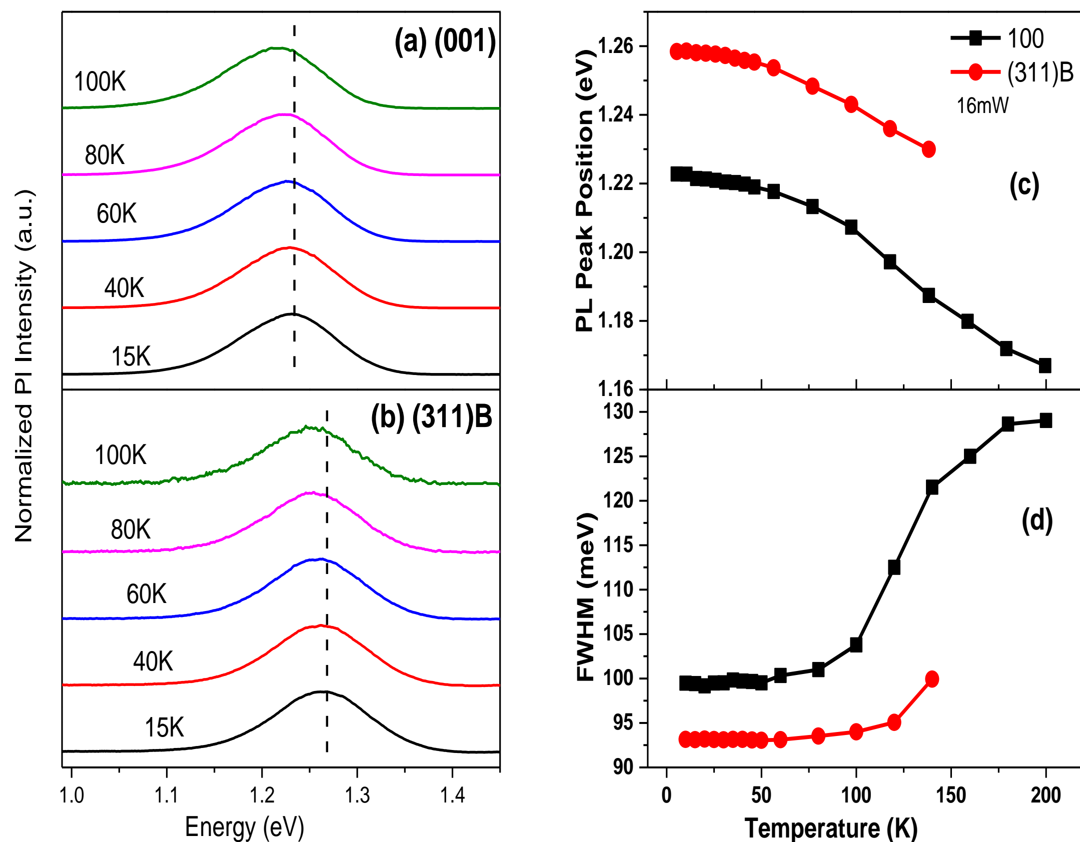


Figure 7. Normalized PL spectra at 16mW as a function of temperature for samples which are grown on (a) (001) and on (b) (311)B GaAs substrates. (c) PL peak energy and (d) FWHM at 16 mW as a function of temperature for (001) and (311)B samples

Figure 7 (d) also shows that the FWHM is similar for both samples with values of 93 and 101 meV for (001) and (311)B direction growth, respectively. These similar values could be explained in terms of the smooth interface of QW as well as the spread of the vertical Bi concentrations profiles as discussed above for HR-XRD diffraction curves.

PL measurements were also carried out on annealed GaAsBi QWs grown on (311)B and (001) oriented GaAs substrates using two different techniques and different conditions as explained previously. It is worth noting that the optical and electronic properties of semiconductor materials are sensitive to the post-growth thermal annealing conditions. However, the influence of annealing procedure on the optical and structural properties of MBE grown GaAsBi QW have not been reported as a function of substrate orientation. The evolution of 10K PL spectra for different annealing temperature conditions are shown in Figure 8 for both substrate

ACCEPTED MANUSCRIPT
Journal of Applied Physics
AIP Publishing
This is the author's peer reviewed, accepted manuscript. However, the online version of record will be different from this version once it has been copyedited and typeset.
PLEASE CITE THIS ARTICLE AS DOI: 10.1063/1.5140447

orientations. The QW emission energy is slightly changed for different annealing temperatures. However, as shown in Figure 8 the PL intensity increases after annealing meaning that the optical quality is improved by both annealing procedures, except the case of (311)B sample which was RTA annealed at 500 °C for 1 min.

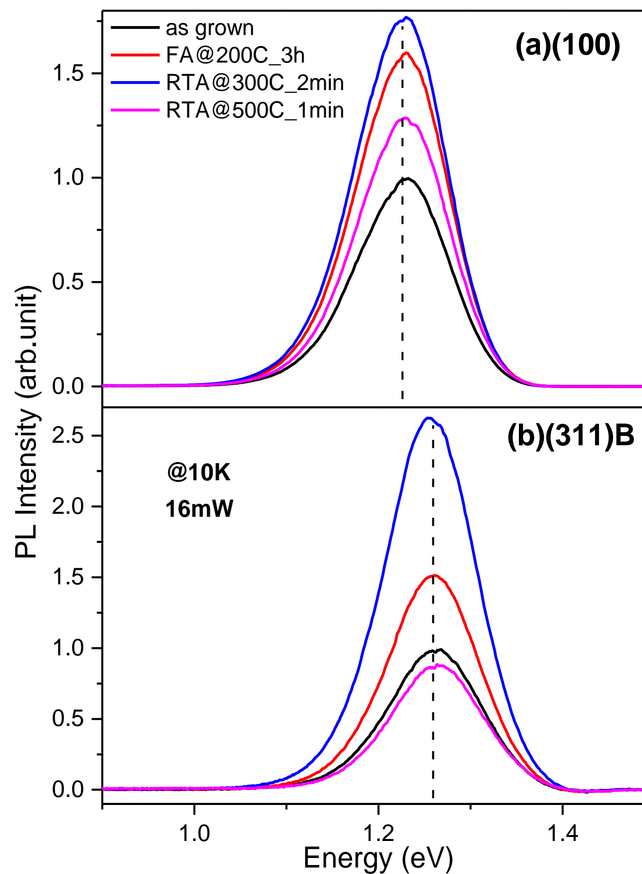


Figure 8. 10 K PL spectra at 16 mW laser power of as-grown and annealed (a) (001) and (b) (311)B $GaAs/GaAs_{0.97}Bi_{0.03}$ QW samples.

The improvement in PL intensity can be explained in terms of decrease in the QW localized states density. Degradation of the QW interfaces with annealing and a decrease of the density of localized defects, due to bismide aggregates or alloy disorder, have been reported to occur during annealing by Mohmad et al. [43] and Mazzucato et al. [44].

As can be seen in Figure 8 (b), there is a significant improvement of the PL intensity of about 2.5 times for the (311)B sample annealed at 300 °C for 2 mins (optimum conditions) while for the (001) sample there is an increase of a factor of ~1.75. However, when both samples were annealed at 700 °C for 30 s (not shown here) the optical quality degraded significantly, and no

ACCEPTED MANUSCRIPT
Journal of Applied Physics
AIP Publishing
This is the author's peer reviewed, accepted manuscript. However, the online version of record will be different from this version once it has been copyedited and typeset.
PLEASE CITE THIS ARTICLE AS DOI: 10.1063/1.5140447

PL emission was detected. This degradation of PL intensity is in accordance with what was observed in other studies [30, 43], where the annealing treatment at temperatures higher than 700°C typically degrades the PL intensity with respect to the as-grown samples, since a very high annealing temperature leads to the activation of additional non-radiative centers. This could be explained by the fact that high annealing temperatures, well above the growth temperature, could lead to a re-distribution of the Bi atoms in the lattice or Bi out-diffusion from the well. The surface damage during the high temperature annealing process could also explain the disappearance of PL emission. As highlighted by Hajer et al., no room temperature PL emission is visible for the annealed samples at 750 ºC and 800 ºC [19] but they observed PL at 20K. On the other hand, appropriate thermal annealing is more efficient to improve the optical quality of alloys without affecting the PL peak wavelength [45].

To assess the samples quality and explain the nonradiative process for the samples grown on the different substrate planes, Arrhenius plots (integrated PL intensities ($I_{PL}$) versus reciprocal temperature) are obtained for a $P_{XEC}$=16mW as shown in Figure 9. Both as-grown and annealed (at 300 ºC for 2 mins) (001) and (311)B GaAsBi QW samples are analysed. The behaviour is classified into thermally activated nonradiative recombination processes. The fits are derived by applying the formalism described in [46, 47].

$$I(T) = I(0)/[1 + C_1 \exp\left(-{}^{E_1}/_{k_B} T\right) + C_2 \exp\left(-{}^{E_2}/_{k_B} T\right)] \tag{1}$$

where I(T) and I(0) are the PL integrated intensity at temperature T and 0K, respectively. $C_1$ and $C_2$ are the non-radiative and radiative recombination probabilities, $k_B$ is the Boltzmann constant, $E_1$ and $E_2$ are the thermal activation energies. A plot of IPL versus 1/ $k_B$ T is shown in Figure 9 and the activation energies obtained by these fittings before and after RTA at 300 ºC for 2 mins. Usman et al. and Zhang et al. found that low concentration of Bi atoms in the GaAs host lattice create potential fluctuation, alloy disorder, clusters and localized pairs [48, 49]. These have different binding energies and configuration, and are classified into two categories depending on their activation energies: (i) the first category with energies ~50 meV is related to alloy disorder [6, 10, 44, 45] and (ii) the second category with energies ranging from 8 meV to 15 energy is assigned to Bi clusters and Bi pairs [38, 46, 44]. The activation energies $E_1$, determined by curve fitting for (001), is 30.0±0.2 meV at low temperatures which is related to alloy disorder caused by Bi incorporation fluctuation [44, 10,45]. The values of $E_1$ and $E_2$ for (001) as-grown are higher than those of (311)B. A smaller thermal activation energy

ACCEPTED MANUSCRIPT
Journal of Applied Physics
AIP Publishing
This is the author's peer reviewed, accepted manuscript. However, the online version of record will be different from this version once it has been copyedited and typeset.
PLEASE CITE THIS ARTICLE AS DOI: 10.1063/1.5140447

means that thermally activated nonradiative recombination can easily occur in samples grown on (311)B than (001) GaAs substrates resulting in a slower drop in the PL intensity of (311)B GaAsBi QW samples as temperature increases than in (001) samples. In particular, for (311)B sample, similar values for activation energy have been reported in our previous work [23]. In contrast, with the annealed sample, the Arrhenius plots provide activation energies of around 16±0.1 and 6.3±1.0 for (001) sample and 10.1±0.1 and 5.1±0.3 meV for (311)B sample.

The drop of the activation energy observed for both annealed samples when compared with as-grown samples could be interpreted as (i) a reduction of the alloy disorder and (ii) an increment of the Bi cluster as discussed before. This, therefore, results in a reduction of non-radiative centers and an enhancement of the PL intensity. These findings seem to agree with the structural changes observed in our HR-TEM data, since the Bi clustering, probably due to the Bi-segregation, become more effective during the annealing process.

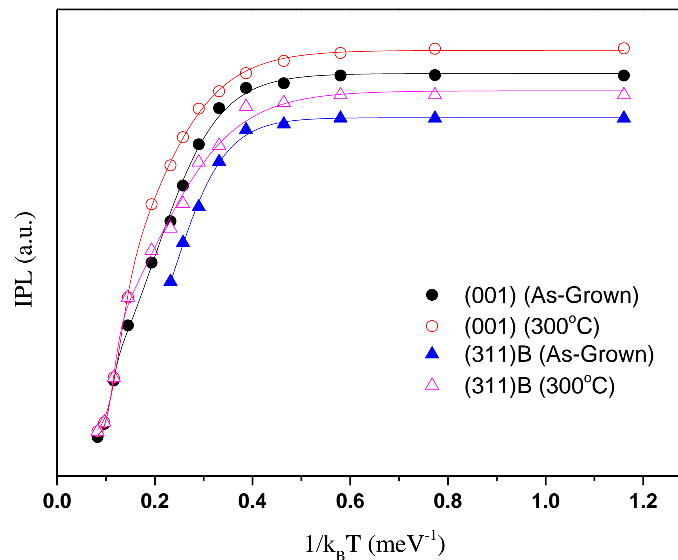


Figure 9: Integrated PL (IPL) intensities at 16 mW of as-grown (001) and (311)B GaAsBi QW and thermally annealed QW at 300 ºC as a function of inverse temperature.

ACCEPTED MANUSCRIPT
Journal of Applied Physics
AIP Publishing
This is the author's peer reviewed, accepted manuscript. However, the online version of record will be different from this version once it has been copyedited and typeset.
PLEASE CITE THIS ARTICLE AS DOI: 10.1063/1.5140447

Table 1: fitting parameters from the measured temperature dependent integrated PL intensities of (001) and (311)B samples**.**

| ***Sample*** | ***$E_1$ (eV)*** | ***$E_2$ (eV)*** |
|---|---|---|
| 001 As-grown | 30 ±0.2 | 10.2±0.8 |
| 001 Annealed | 16±0.1 | 6.3±1.0 |
| (311)B As-grown | 25±1.5 | 7.5±0.8 |
| (311)B Annealed | 10.1±0.1 | 5.1±0.3 |

**Conclusions**

In conclusion, the effects of RTA and FA upon the HR-XRD, TEM and PL measurements from GaAsBi single quantum well with 3% Bi grown on (001) and (311)B GaAs substrates were investigated. The HR-XRD results reveal a very small difference between the as-grown and annealed samples and the Bi composition is not uniform in the epilayer and in the QW layer. The HR-XRD spectra demonstrated that the Bi concentration inhomogeneity is more pronounced for (311)B than (001) samples. The HRTEM images show evidence of Bi-segregation, which is more pronounced in (001) samples after annealing. The single QW shows a structural stability in terms of thickness for the optimum annealing temperature of 300 °C for 2 mins. RTA is found to be a more effective method to improve the PL intensity than FA, which could be due to a reduction of structural defects in the samples. The optimum annealing condition is determined to be 300°C for 2 mins for all studied samples regardless of the substrate orientations. The increase of PL intensity in annealed samples was interpreted in terms of PL activation energies, with a reduction of the alloy disorder and an increase of the Bi cluster.

**Acknowledgments:** We acknowledge J. Puustinen and J. Hilska from the Optoelectronics Research Centre, Tampere University, for fabricating the epitaxial samples". YGG and HVAG acknowledge the financial support from Fundação de Amparo a Pesquisa do Estado de São Paulo (FAPESP) (grant numbers 18/01808-5, 16/10668-7, and 19/07442-5). JFF would to like to thank the Brazilian agencies CNPq (grant number: 430470/2018-5), FAPDF (grant number:193.001.757/2017), for financial support and the research scholarship. HCJ acknowledge the financial support from Fundação Carlos Chagas Filho de Amparo à Pesquisa do Estado do Rio de Janeiro (FAPERJ). M.Gunes acknowledges TUBITAK project no: 115F063.

ACCEPTED MANUSCRIPT
Journal of Applied Physics
AIP Publishing
This is the author's peer reviewed, accepted manuscript. However, the online version of record will be different from this version once it has been copyedited and typeset.
PLEASE CITE THIS ARTICLE AS DOI: 10.1063/1.5140447

**References**

[1] S. Francoeur, M.-J. Seong, A. Mascarenhas, S. Tixier, M. Adamcyk, and T. Tiedje, Appl. Phys. Lett. 82, 3874 (2003).

[2] V. V. Pacˇebutas, K. Bertulis, G. Aleksejenko, and A. Krotkus, J. Mater.Sci.: Mater. Electron. 20, S363 (2009).

[3] B. Fluegel, S. Francoeur and A. Mascarenhas, Phys. Rev. Lett. 97, 067205 (2006).

[4] Z. Batool, K. Hild, T. J. C. Hosea, X. Lu, T. Tiedje, and S. J. Sweeney,J. Appl. Phys. 111, 113108 (2012).

[5] A. Chernikov, V. Bornwasser, M. Koch, S. W. Koch, X. Lu, S. R. Johnson, D. A. Beaton, T. Tiedje, and S. Chatterjee, Semicond. Sci.Technol. 27, 085012 (2012).

[6] S. Imhof, C. Wagner, A. Thränhardt, A. Chernikov, M. Koch, N. S. Koster, S. Chatterjee, S. W. Koch, O. Rubel, X. Lu, S. R. Johnson, D. A. Beaton, and T. Tjedje, Appl. Phys. Lett. 98, 161104 (2011).

[7] M. A. G. Balanta, J. Kopaczek, V. O. Gordo, B. H. B. Santos, A. D. Rodrigues, H. V. A. Galeti, R. D. Richards, F. Bastiman, J. P. R. David, R. Kudrawiec, and Y. G. Gobato, Journal of Physics. D, Applied Physics, 49, 355104, (2016).

[8] A. H. Carvalho, V. Orsi Gordo, H. V. A. Galti, Y. G. Gobato, M. P. F. de Godoy, R. Kudrawiec, O. M. Lemine, and M. Henini, Journal of Physics. D, Applied Physics 47, 075103(2014).

[9] I. A. Buyanova, W. M. Chen, and C. W. Tu, Solid-State Electron. 47, 467 (2003).

[10] S. Imhof, A. Thräanhardt, A. Chernikov, M. Koch, N. S. Koster, K. Kolata,S. Chatterjee, S. W. Koch, X. Lu, S. R. Johnson, D. A. Beaton, T. Tiedje, and O. Rubel, Appl. Phys. Lett. 96, 131115 (2010).

[11] X. Lu, D. A. Beaton, R. B. Lewis, T. Tiedje, and Y. Zhang, Appl. Phys.Lett. 95, 041903 (2009).

[12] B. Čechavičius, R. Adomavičius, A. Koroliov, and A. Krotkus. Semicond. Sci. and Technol. 26, 085033 (2011)

[13] R. B. Lewis, M. Masnadi-Shirazi, and T. Tiedje, Appl. Phys. Lett. 101, 082112 (2012).

[14] R. Butkutė, V. Pačebutas, B. Čechavičius, R. Adomavičius, A. Koroliov, and A. Krotkus, Phys. Status Solidi C 9, 1614 (2012).

[15] M. Henini, J. Ibáñez, M. Schmidbauer, M. Shafi, S. V. Novikov, L. Turyanska, S. I. Molina, D. L. Sales, M. F. Chisholm, and J. Misiewicz, Appl. Phys. Lett. 91, 251909 (2007).

ACCEPTED MANUSCRIPT
Journal of Applied Physics
AIP Publishing
This is the author's peer reviewed, accepted manuscript. However, the online version of record will be different from this version once it has been copyedited and typeset.
PLEASE CITE THIS ARTICLE AS DOI: 10.1063/1.5140447

[16] J. F. Rodrigo, D.L. Sales, M. Shafi, M. Henini, L. Turyanska, S. Novikov, and S.I. Molina, Applied Surface Science 256, 5688 (2010).

[17] M. K. Shakfa, D. Kalincev, X. Lu, S. R. Johnson, D. A. Beaton, T. Tiedje, A. Chernikov, S. Chatterjee, and M.Koch, Journal of Applied Physics 114, 164306 (2013).

[18] H. Makhloufi, P. Boonpeng, S. Mazzucato, J. Nicolai, A. Arnoult, T. Hungria, G. Lacoste, C. Gatel, A. Ponchet, H. Carrère, X. Marie, and C. Fontaine, Nanoscale Res. Lett. 9, 123 (2014).

[19] L. Yue, Y. Song, X. Chen, Q. Chen, W. Pan, X. Wu, J. Liu, L. Zhang, J. Shao, and S. Wang, Journal of Alloys and Compounds, 695, 753 (2017) .

[20] Y. Tominaga, Y. Kinoshita, G. Feng, K. Oe, and M. Yoshimoto, Applied Physics Lett. 93,131915 (2008).

[21] D. Fan, P. C. Grant, S.-Q. Yu, V. G. Dorogan, X. Hu, Z. Zeng, C. Li, M. E. H., M. Benamara, Y. I. Mazur, G. J. Salamo, S. R. Johnson, and Z. M. Wang, Journal of Vacuum Science & Technology B, 31, 03C105 (2013).

[22] P. K. Patil, F. Ishikawa, and S. Shimomura, Superlattices and Microstructures, 100, 10 (2016).

[23] G. A. Prando, V. Orsi Gordo, J. Puustinen, J. Hilska, H. M. Alghamdi, G. Som, M. Gunes, M. Akyol, S Souto, A. D. Rodrigues, H. V. A. Galeti, M. Henini, Y. Galvão Gobato, and M. Guina. Semicond. Sci. Technol., 33, 084002 (2018).

[24] M. Gunes, M. O. Ukelge, O. Donmez, A. Ero, C. Gumus, H. Alghamdi, H. V. A. Galeti, M. Henini, M. Schmidbauer, J. Hilska, J. Puustinen, and M. Guina, Semiconductor Science and Technology, 33, 12 (2018).

[25] M. V. Maksimov, D. S. SizovA. G. Makarov, I. N. Kayander, L. V. Asryan, A. E. Zhukov, V. M. Ustinov, N. A. Cherkashin, N. A. Bert, N. N. Ledentsov, and D. Bimberg, Semiconductors 38, 10 1207(2004).

[26] E. V. K. Rao, A. Ougazzaden, Y. Le Bellego, and M. Juhe, Appl. Phys.Lett. 72, 1409 (1998).

[27] L. Grenouillet, C. Bru-Chevallier, G. Guillot, P. Gilet, P. Ballet, P.Duvaut, G. Rolland, and A. Million, J. Appl. Phys. 91, 5902 (2002).

[28] I. Moussa, H. Fitouri, Z. Chine, A. Rebey, and B. El Jani, Semicond. Sci.and Tech. 23, 125034 (2008).

[29] Z. Chine, H. Fitouri, I. Zaied, A. Rebey, and B. El Jani. Semicond.Sci.and Tech. 25, 065009 (2010).

[30] P. C. Grant, D. Fan, A. Mosleh, and S.-Q. Yu, Journal of Vacuum Science & Technology B, 32, 02C119 (2014).

ACCEPTED MANUSCRIPT
Journal of Applied Physics
AIP Publishing
This is the author's peer reviewed, accepted manuscript. However, the online version of record will be different from this version once it has been copyedited and typeset.
PLEASE CITE THIS ARTICLE AS DOI: 10.1063/1.5140447

[31] N. Baladés, D. L. Sales, M. Herrera, C. H. Tan, Y. Liu, R. D. Richards, and S. I. Molina, Nanoscale Research Letters, 13, 125 (2018).

[32] G. Pettinari, A. Polimeni, M. Capizzi, J. H. Blokland, P. C. M. Christianen, J. C. Maan, E C. Young, and T. Tiedje, Appl. Phys. Lett., 92, 262105 (2008).

[33] S. Francouer, S. Tixier, E.C. Young, T. Tiedje, and A. Mascarenhas, Physics Review B. 77, 085209 (2008).

[34] T. Schmidt, K. Lischka, and W. Zulehner, Phys. Rev. B 45, 8989 (1992).

[35] R. Kudrawiec, M. Syperek, P. Poloczek, J. Misiewicz, R. H. Mari, M. Shafi, M. Henini, Y. Galvão Gobato, S. V. Novikov, J. Ibáñez, M. Schmidbauer, *and* S. I. Molina, J. Appl. Phys. 106, 023518 (2009).

[36] S. Mazzucato, H. Lehec, H. Carrère, H. Makhloufi, A. Arnoult, C. Fontaine, T. Amand, and X. Marie, Nanoscale Res. Lett., 9, 19 (2014).

[37] Y. P. Varshni, Physica, 34, 149 (1967).

[38] O. Donmez, A. Erol, M. C. Arikan, H. Makhloufi, A. Arnoult, and C. Fontaine, Semicond. Sci. Technol., 30, 94016 (2015).

[39] A. R. Mohmad, F. Bastiman, C. J. Hunter, R. D. Richards, S. J. Sweeney, J. S. Ng, J. P. R. David, and B. Y. Majlis, Phys. Status Solidi Basic Res., 251, 1276 (2014).

[40] T. Wilson, N. P. Hylton, Y. Harada, P. Pearce, D. Alonso-Álvarez, A. Mellor, R. D. Richards, J. P. R. David, and N. J. Ekins-Daukes, Sci. Rep., 8, 6457 (2018).

[41] Y. I. Mazur, V. G. Dorogan, M. Benamara, M. E. Ware, M. Schmidbauer, G. G. Tarasov, S. R. Johnson, X. Lu, S-Q Yu, T. Tiedje, and G. J. Salamo, J. Phys. D: Appl. Phys., 46, 065306 (2013) .

[42] Y. I. Mazur, V. G. Dorogan, M. Schmidbauer, G. G. Tarasov, S. R. Johnson, X. Lu, M. E. Ware, S. Q.Yu, T. Tiedje, and G. J. Salamo, J. Appl. Phys., 113 144308 (2013)..

[43] A.R. Mohmad, F. Bastiman, C.J. Hunter, R. Richards, S.J. Sweeney, J.S. Ng, and J.P.R David, Applied Physics Letters. 101, 012106 (2012).

[44] S. Mazzucato, P. Boonpeng, H. Carrère, D. Lagarde, A. Arnoult, G. Lacoste, T. Zhang, A. Balocchi, T. Amand, X. Marie, and C. Fontaine, Semiconductor Science and Technology. 28, 022001 (2013).

[45] M. Yoshimoto, M. Itoh, Y. Tominaga, and K. Oe, J. Cryst. Growth, 378, 73 (2013).

[46] S. M. Olsthoorn, F. A. J. M. Driessen, A. P. A. M. Eijkelenboom, and L. J. Giling Journal of Applied Physics 73 (1 l), 7798 (1993).

Journal of Applied Physics
ACCEPTED MANUSCRIPT
AIP Publishing
This is the author's peer reviewed, accepted manuscript. However, the online version of record will be different from this version once it has been copyedited and typeset.
PLEASE CITE THIS ARTICLE AS DOI: 10.1063/1.5140447

[47] H. D. Sun, S. Calvez, M. D. Dawson, J. A. Gupta, G. C. Aers, and G. I. Sproule, Applied Physics Letters, 89, 101909 (2006).

[48] M. Usman, C. A. Broderick, A. Lindsay, and E. P. O'Reilly, Phys. Rev. B 84, 245202 (2011).

[49] Y. Zhang, A. Mascarenhas, and L.W. Wang, Phys. Rev. B, 71, 155201 (2005).

[50] M. Wu, E. Luna, J. Puustinen, M. Guina, and A. Trampert, Nanotechnology, 25, 205605 (2014).

[51] M.A.G. Balanta, V. Orsi Gordo, A.R.H. Carvalho, J. Puustinen, H.M. Alghamdi, M. Henini, H.V.A. Galeti, M. Guina, and Y. Galvão Gobato. Journal of Luminescence 182, 49–52 (2017).

[52] O.M. Lemine, A. Alkaoud, H.V. Avanço Galeti, V. Orsi Gordo, Y. Galvão Gobato, Houcine Bouzid, A. Hajry, and M. Henini. Superlattices and Microstructures 65, 48–55 (2014).

[53] S. Tixier, M. Adamcyk, T. Tiedje, S. Francoeur, A. Mascarenhas, Peng Wei, and F. Schiettekatte. Applied Physics Letters. 82, 2245 (2003).

[54] see http://www.ioffe.ru/SVA/NSM/Semicond/GaAs/mechanic.html#Elastic

ACCEPTED MANUSCRIPT
Journal of Applied Physics
AIP Publishing
This is the author's peer reviewed, accepted manuscript. However, the online version of record will be different from this version once it has been copyedited and typeset.
PLEASE CITE THIS ARTICLE AS DOI: 10.1063/1.5140447

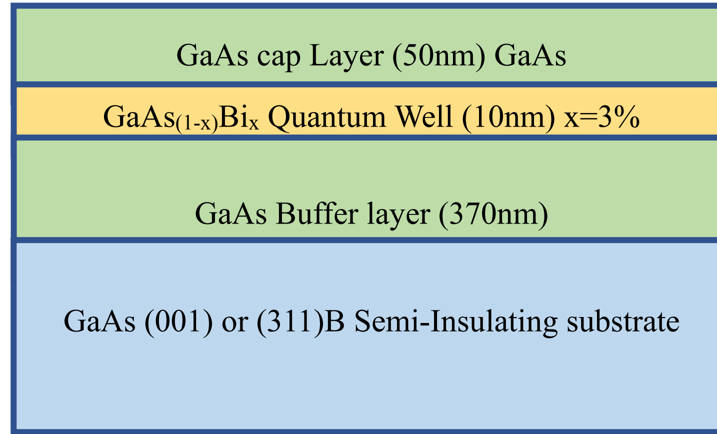


Figure 1: Schematic diagram of GaAsBi/GaAs SQW sample grown on (001) and (311)B GaAs substrates.

ACCEPTED MANUSCRIPT
Journal of Applied Physics
AIP Publishing
This is the author's peer reviewed, accepted manuscript. However, the online version of record will be different from this version once it has been copyedited and typeset.
PLEASE CITE THIS ARTICLE AS DOI: 10.1063/1.5140447

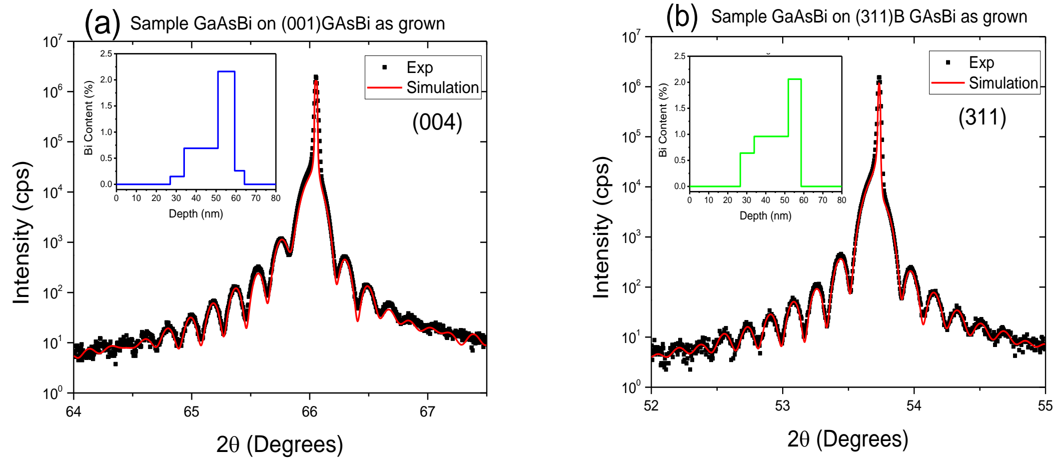


Figure 2. Experimental (black dots) and simulated (solid lines) 2θ-ω scans of samples grown on (a) (001) GaAs and (b) (311)B GaAs substrates. The insets show the vertical Bi concentration profile which was used in the simulations.

ACCEPTED MANUSCRIPT
Journal of Applied Physics
AIP Publishing
This is the author's peer reviewed, accepted manuscript. However, the online version of record will be different from this version once it has been copyedited and typeset.
PLEASE CITE THIS ARTICLE AS DOI: 10.1063/1.5140447

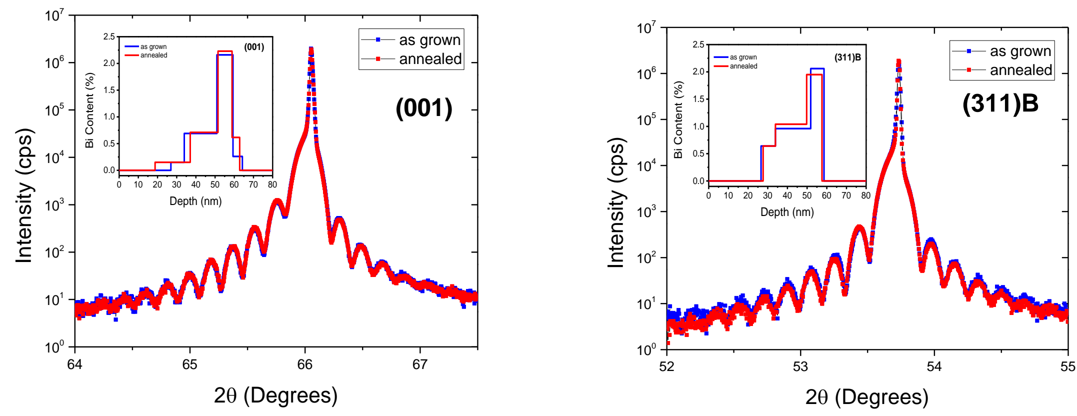


Figure 3. 2θ-ω scans of as-grown and RTA annealed samples around the symmetrical (a) (004) and (b) (311)B Bragg reflections of the GaAs substrate. The corresponding insets show the Bi concentration profiles used in the best data fits for all four samples. Reproduced with permission from Semiconductor Science and Technology 33, 124015 (2018). ©IOP Publishing. Reproduced with permission. All rights reserved.

Journal of Applied Physics
ACCEPTED MANUSCRIPT
AIP Publishing
This is the author's peer reviewed, accepted manuscript. However, the online version of record will be different from this version once it has been copyedited and typeset.
PLEASE CITE THIS ARTICLE AS DOI: 10.1063/1.5140447

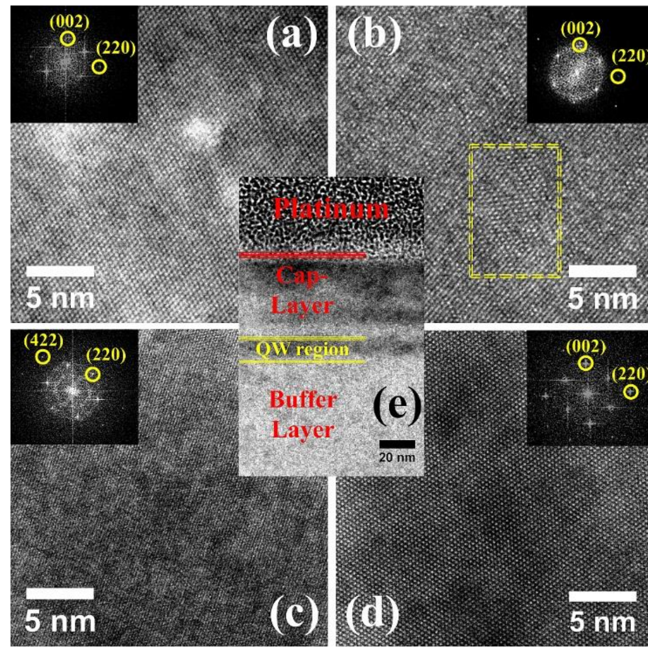


Figure 4. High-Resolution TEM micrographs obtained from the GaAsBi/GaAs interface region: (a) as-grown (001) sample, (b) annealed (001) sample, (c) as-grown (311)B sample and (d) annealed (311)B sample. In (a), (b) and (d), the insets show the results of the fast Fourier transform (FFT) image reconstructions along the [110] zone axis, respectively, while in (c) the FFT image is along the [$\bar{1}$11] zone axis. The dashed line in (b) indicates a region of structural relaxation after annealing. (e) annealed (311)B sample at lower magnification; the sample surface is between platinum and cap-layer. The substrates are located on the bottom of image (a) an (b) and left side of image (c) and (d).

ACCEPTED MANUSCRIPT
Journal of Applied Physics
AIP Publishing
This is the author's peer reviewed, accepted manuscript. However, the online version of record will be different from this version once it has been copyedited and typeset.
PLEASE CITE THIS ARTICLE AS DOI: 10.1063/1.5140447

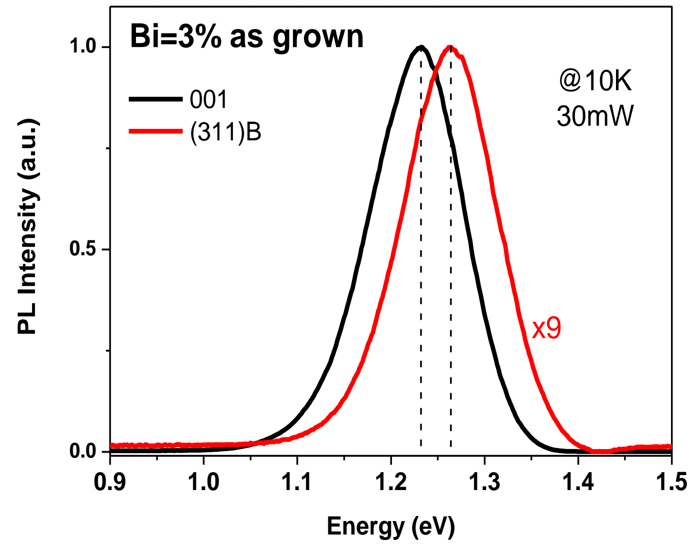


Figure 5. Normalised PL spectra for as-grown samples on (001) and (311)B GaAs substrate.

ACCEPTED MANUSCRIPT
Journal of Applied Physics
AIP Publishing
This is the author's peer reviewed, accepted manuscript. However, the online version of record will be different from this version once it has been copyedited and typeset.
PLEASE CITE THIS ARTICLE AS DOI: 10.1063/1.5140447

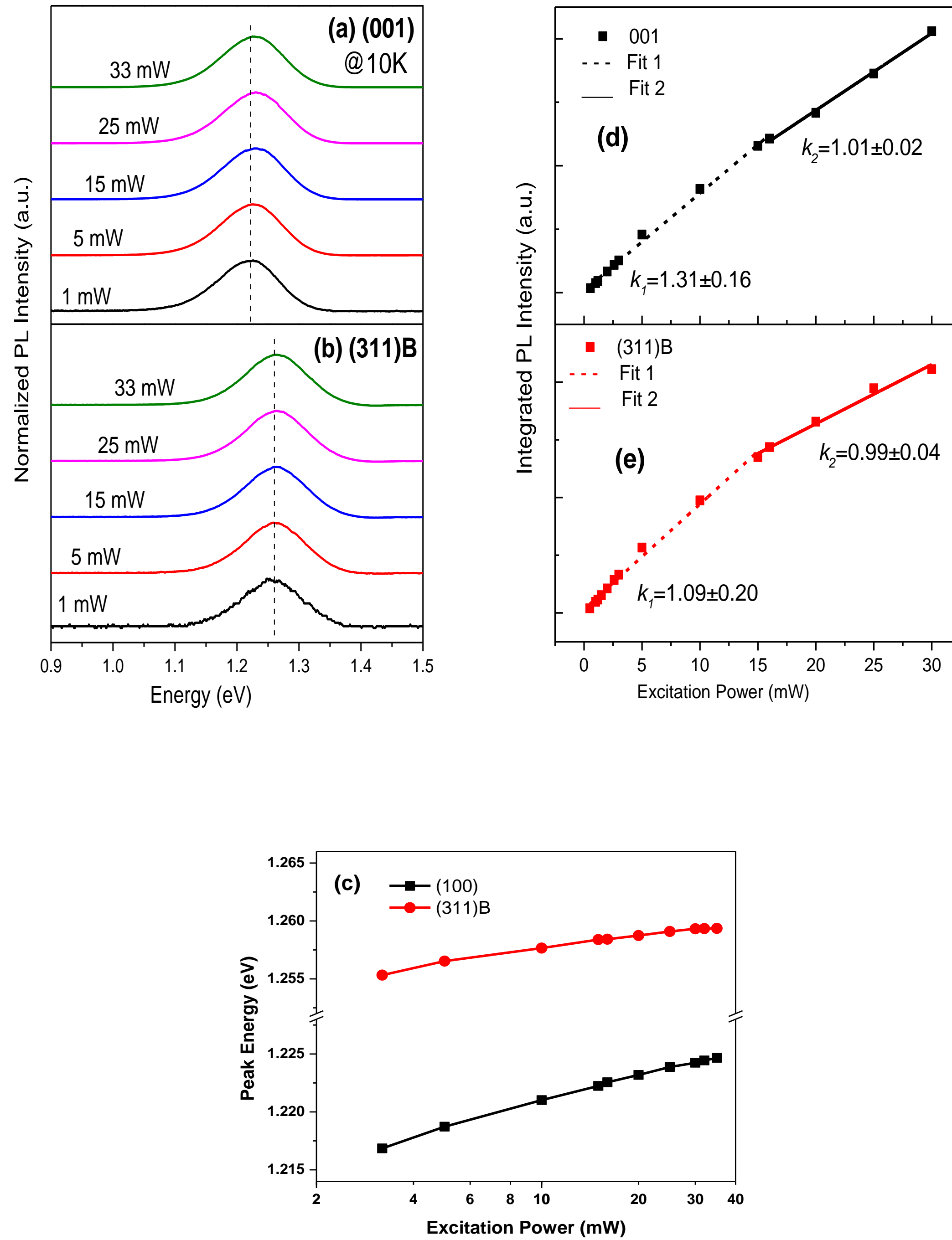


Figure 6. Normalized PL spectra at 10 K for different $P_{EXC}$ for (a) (001) and (b) (311)B as-grown samples. (c) PL peak energy as a function of $P_{EXC}$ for (001) and (311)B samples. Integrated PL intensity (IPL) as a function of $P_{EXC}$ for (d) (001) and (e) (311)B samples at 10K. The solid and dashed lines represent the fitting using equation: $I_{PL} = \beta P_{EXC}^{k}$

ACCEPTED MANUSCRIPT
Journal of Applied Physics
AIP Publishing
This is the author's peer reviewed, accepted manuscript. However, the online version of record will be different from this version once it has been copyedited and typeset.
PLEASE CITE THIS ARTICLE AS DOI: 10.1063/1.5140447

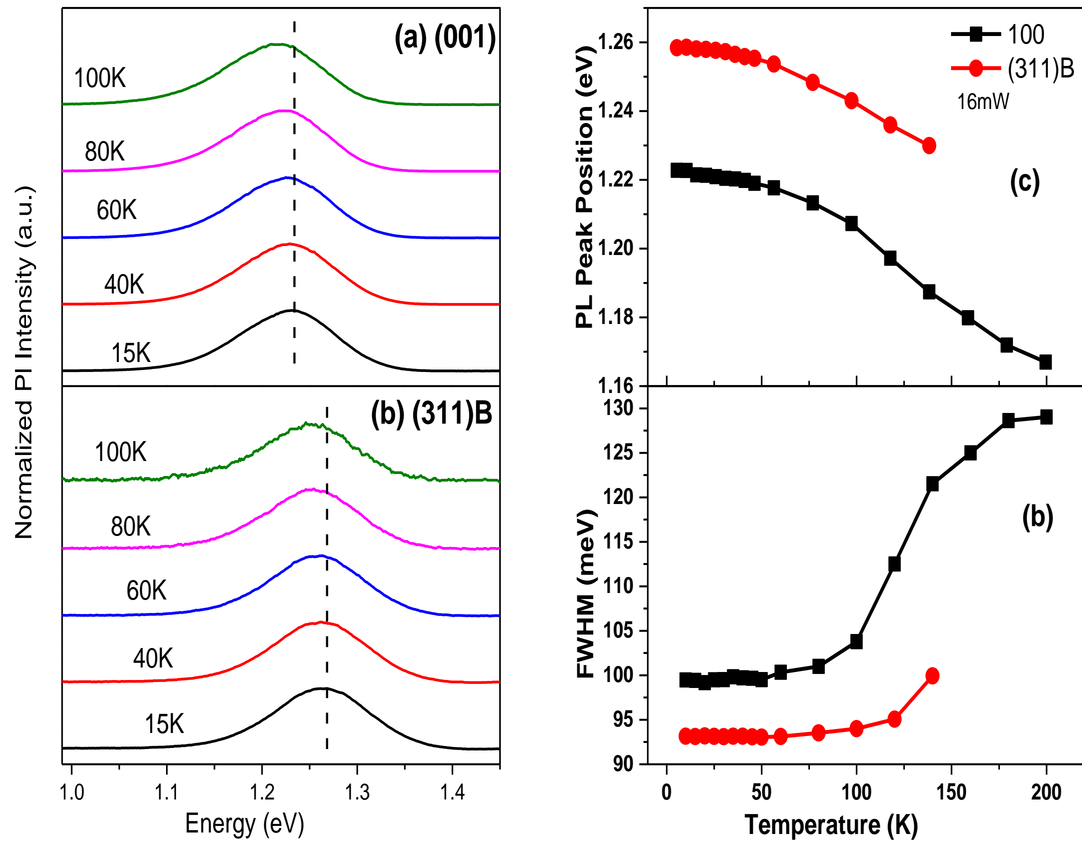


Figure 7. Normalized PL spectra at 16mW as a function of temperature for samples which are grown on (a) (001) and on (b) (311)B GaAs substrates. (c) PL peak energy and (d) FWHM at 16 mW as a function of temperature for (001) and (311)B samples

Journal of Applied Physics
ACCEPTED MANUSCRIPT
AIP Publishing
This is the author's peer reviewed, accepted manuscript. However, the online version of record will be different from this version once it has been copyedited and typeset.
PLEASE CITE THIS ARTICLE AS DOI: 10.1063/1.5140447

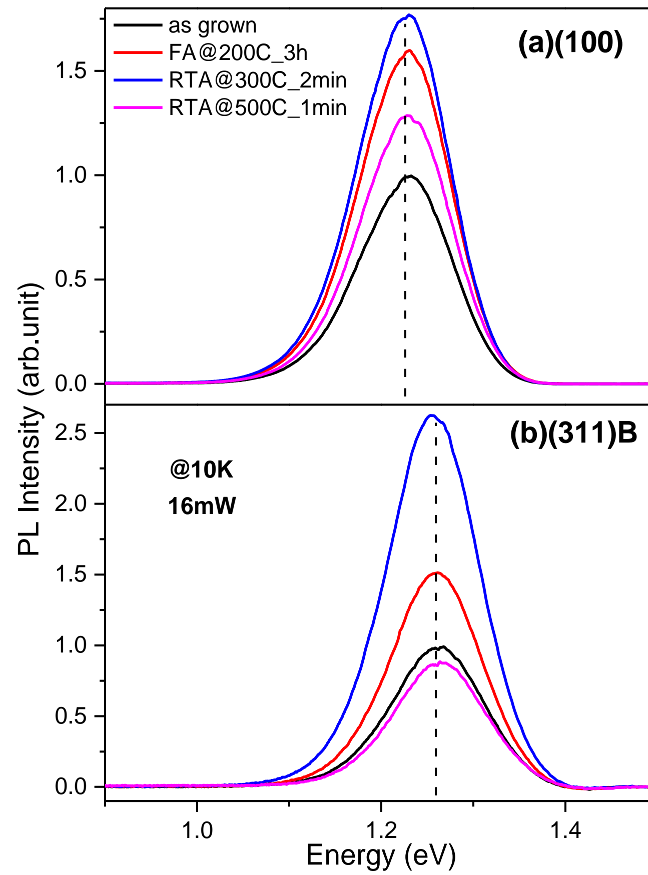


Figure 8. 10 K PL spectra at 16 mW laser power of as-grown and annealed (a) (001) and (b) (311)B $GaAs/GaAs_{0.97}Bi_{0.03}$ QW samples.

ACCEPTED MANUSCRIPT
Journal of Applied Physics
AIP Publishing
This is the author's peer reviewed, accepted manuscript. However, the online version of record will be different from this version once it has been copyedited and typeset.
PLEASE CITE THIS ARTICLE AS DOI: 10.1063/1.5140447

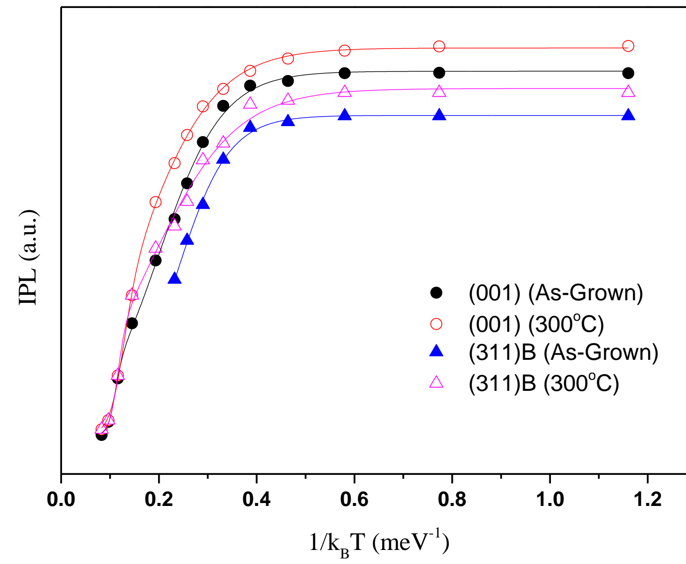


Figure 9: Integrated PL (IPL) intensities at 16 mW of as-grown (001) and (311)B GaAsBi QW and thermally annealed QW at 300 °C as a function of inverse temperature.